Title

Muscle immobilization delays abrupt change in myoglobin saturation at onset of muscle contraction

Journal

The Journal of Physical Fitness and Sports Medicine, 11(2)

ISSN

2186-8131

Authors

Takakura, Hisashi
Yamada, Tatsuya
Furuichi, Yasuro
et al.

Publication Date

2022-03-25

DOI

10.7600/jpfsm.11.87

Peer reviewed

J Phys Fitness Sports Med, 11 (2): 87-96 (2022)
DOI: 10.7600/jpfsm.11.87

JPFSM: ***Regular Article***

Muscle immobilization delays abrupt change in myoglobin saturation at onset of muscle contraction

Hisashi Takakura[1], Tatsuya Yamada[2], Yasuro Furuichi[3], Takeshi Hashimoto[4], Satoshi Iwase[5], Thomas Jue[6] and Kazumi Masuda[7*]

[1] *Faculty of Health and Sports Science, Doshisha University, 1-3 Tatara Miyakodani, Kyotanabe, Kyoto 610-0394, Japan*
[2] *Department of Cell Biology, Johns Hopkins University School of Medicine, Baltimore, MD 21205, USA*
[3] *Department of Health Promotion Science, Tokyo Metropolitan University, 1-1 Minami-Osawa, Hachioji, Tokyo 192-0397, Japan*
[4] *Faculty of Sports and Health Science, Ritsumeikan University, 1-1-1 Noji-higashi, Kusatsu, Shiga 525-8577, Japan*
[5] *Department of Physiology, Aichi Medical University, 1-1 Yazakokarimata, Nagakute, Aichi 480-1195, Japan*
[6] *Department of Biochemistry and Molecular Medicine, University of California Davis, Davis 95616-8635, USA*
[7] *Faculty of Human Sciences, Kanazawa University, Kakuma-machi, Kanazawa, Ishikawa 920-1192, Japan*

Received: May 21, 2021 / Accepted: September 8, 2021

Abstract Hindlimb immobilization (IM) produces a decrease in functional oxidative capacity as well as morphological changes in muscles. However, the effect of IM on the mechanism of O_2 supply to mitochondria in muscle tissue during muscle contraction is unknown, especially the contribution of myoglobin (Mb) to mitochondrial respiration. This study investigated whether IM causes a delayed response of intracellular Mb saturation ($S_{mb}O_2$) and decreased muscle oxygen uptake ($m\dot{V}O_2$) due to elevated intracellular oxygen tension ($P_{mb}O_2$) in contracting muscles using a rat hindlimb perfusion model. Three-week IM decreased the O_2 release rate from Mb at the onset of muscle contraction (IM: 3.2 ± 0.9 vs. control (Con): 7.5 ± 2.9 10^{-2} μmol g^{-1} min^{-1}; $p < 0.05$) and state 3 of mitochondrial respiration in muscle tissue (IM: 0.021 ± 0.006 vs. Con: 0.030 ± 0.009 10^{-3} μM g^{-1} sec^{-1}; $p < 0.05$). Despite the increase in $m\dot{V}O_2$, the steady-state level of $S_{mb}O_2$ was higher during muscle contraction in the IM group, resulting in elevated $P_{mb}O_2$ (IM: 4.2 ± 1.0 vs. Con: 2.1 ± 1.0 mmHg; $p < 0.05$). In conclusion, IM decreased the O_2 release rate from Mb; this alteration could be associated with mitochondrial dysfunction. These changes within muscle cells may be related to the delayed tissue response seen with near-infrared spectroscopy at the onset of muscle contraction.

Keywords : hindlimb perfusion, myoglobin, immobilization, mitochondrial respiration

Introduction

Animal models of hindlimb immobilization (IM), tail suspension, and denervation are frequently used to study the adaptation of skeletal muscle to chronic disuse. These models produce alteration in muscle metabolism as well as in muscle morphology[1-5]. How hindlimb immobilization affects the oxidative phosphorylation capacity remains unclear. To date, *in vitro* biochemical and histochemical analyses have been used extensively to study the change in protein abundance, mitochondrial volume, and oxidative enzyme activity due to chronic disuse. However, only studying the change in integrated muscle oxidative capacity under physiological conditions *in vivo* will clarify the relationship between muscle disuse and oxidative capacity.

For the evaluation of muscle oxidative capacity *in vivo*, some studies have used the transient response from rest to exercise of $\dot{V}O_2$ (oxygen uptake) kinetics and muscle deoxygenation kinetics measured using near-infrared spectroscopy (NIRS)[6-8]. Indeed, Convertino et al.[6] revealed slowed-down $\dot{V}O_2$ kinetics in an upright position after bed rest deconditioning, suggesting a decrease in O_2 transport/utilization capacity during the transient phase. Similarly, at the peripheral tissue level, 20 days of the unilateral lower limb unloading model delayed the time constant of NIRS deoxygenation kinetics during muscle contraction[7], and the 21-day forearm IM prolonged the time constant for phosphocreatine recovery after exercise[8]. These previous studies suggested that a delay in transient response at the onset of contraction was caused by a decrease in muscle oxidative capacity[7,8]. Recently, we have succeeded in detecting myoglobin (Mb) deoxygenation kinetics using NIRS during muscle contraction[9,10]. This experimental model can be used to investigate intracellular O_2 dynamics during muscle contraction. Furthermore, the high time resolution of the NIRS methodology can better follow the transient response from rest to contraction than nuclear

*Correspondence: masudak@staff.kanazawa-u.ac.jp

magnetic resonance (NMR) techniques[11]. Our previous study showed that endurance training increased the O_2 release rate from Mb to the mitochondria at the onset of muscle contraction and contributed to faster $\dot{V}O_2$ kinetics in endurance trained muscles[12].

Although the change in physical activity levels undoubtedly influences transient response of various physiological parameters involved in oxidative capacity, it remains unclear whether the O_2 release rate from Mb is decreased in the immobilized skeletal muscle with decreased muscle oxidative capacity. A previous study reported that a significant decrease in the state 3 respiratory rate in the mitochondria isolated from the gastrocnemius muscle was observed after 4 weeks of hindlimb suspension[5]. Moreover, considering that the O_2 release rate from Mb is closely related to the mitochondrial respiration rate[9,13], the IM might cause a decrease in the O_2 release rate from Mb at the transient phase from rest to muscle contraction. Therefore, the purpose of the present study was to examine the effect of IM on the O_2 release rate from Mb and intracellular O_2 tension based on O_2 saturation of Mb ($S_{mb}O_2$) and intracellular O_2 tension ($P_{mb}O_2$) kinetics during muscle contraction employing a hemoglobin (Hb)-free rat hindlimb perfusion model.

Materials and Methods

Experimental animals and preparation of hindlimb perfusion

Twenty-seven male Wistar rats were employed as subjects. All were housed in a temperature-controlled room at 23 ± 2°C with a 12-h light–dark cycle and maintained on a commercial diet with water ad libitum. The procedures conformed to the "Fundamental Guidelines for Proper Conduct of Animal Experiment and Related Activities in Academic Research Institutions" (published by the Ministry of Education, Culture, Sports, Science and Technology, Japan) and was approved by the Ethics Committee for Animal Experimentation of Kanazawa University (Protocol AP-101636).

Six-week-old Wistar rats were divided randomly into control (Con) and IM groups. The IM group had their left hindlimbs immobilized at full plantar flexion using a thermoplastic cast (PritonX, Alcare, Tokyo, Japan), while right limbs were allowed to move freely. The thermoplastic cast was wrapped around each rat, from the torso to the toe of the left hindlimb, for 3 weeks. The fixation was checked daily.

After 3 weeks (at age 9 weeks), hindlimb perfusion was performed in each group (Con group: 257–295 g body weight (BW), IM group: 206–229 g BW; n = 6 in each group). All surgical procedures were performed under anaesthesia with intraperitoneal injection (*i.p.*) injection of medetomidine (0.3 mg/kg), midazolam (4 mg/kg), and butorphanol (5 mg/kg). Preparation of isolated rat hindlimb and the perfusion apparatus are described in a previous report[9,10]. The abdominal wall was first incised from the pubic symphysis to the xiphoid process. The spermary, testis, and inferior mesenteric arteries and veins were ligated, and the spermaries, testes, and part of the descending colon were excised, together with contiguous adipose tissue. The caudal artery and internal iliac artery and vein were also ligated. Ligatures were placed around the neck of the bladder, the anterior prostate, and the prostate. The vessels that supply the subcutaneous region were also ligated. Following these ligations, the inferior epigastric, iliolumbar, and renal arteries and veins were ligated as well as the coeliac axis and portal vein. A further ligature was placed around the tail. After surgery, euthanasia was performed by a 1 M KCl solution injected directly into the heart. An Hb-free Krebs-Henseleit buffer (NaCl, 118 mM; KCl, 5.9 mM; KH_2PO_4, 1.2 mM; $MgSO_4$, 1.2 mM; $CaCl_2$, 1.8 mM; $NaHCO_3$, 20 mM; Glucose, 15 mM) was perfused into the abdominal aorta in flow-through mode, at a constant flow rate.

In order to adjust the perfusion pressure to approximately 80.0 mmHg, the flow rate was set to 22.0 ± 0.0 ml/min in the Con group and 19.2 ± 1.5 ml/min in the IM group. In this condition, the average perfusion pressures were 80.9 ± 7.2 mmHg in the Con group and 79.9 ± 4.7 mmHg in the IM group. No symptom of edema in the hindlimb was confirmed at the given flow rate. After cannulating into the abdominal aorta, the contralateral (right hindlimb) common iliac artery was ligated. The Krebs-Henseleit buffer containing heparin (1000 U/L) was perfused into the hindlimb for 10 min from the beginning of the perfusion to prevent blood clotting and to wash out blood from the hindlimb[9,10].

The perfusate and muscle temperature were maintained at 37°C. The rat hindlimb was perfused with buffer equilibrated with 95% O_2 + 5% CO_2 for 30 min before and throughout the exercise protocol. The presence of CO_2 maintained the pH between 7.3 and 7.4. The effluent was collected from the inferior vena cava in order to measure $m\dot{V}O_2$.

Twitch contraction protocol

The nerve stimulation protocol followed our previous methods[9,10]. The sciatic nerve of the left hindlimb was then exposed and connected to two parallel stainless steel wire electrodes (Unique Medical, Tokyo, Japan) and the Achilles tendon was connected to a sensitive strain gauge with a string (MLT500/D, AD Instrument, Castle Hill, NSW, Australia). Stimulation via the sciatic nerve consisted of a single square wave (delay, 10 μsec; duration, 1 msec) controlled by an electrostimulator system (Model RU-72, Nihon Koden, Tokyo, Japan). The stimulation pulse was 1 Hz in frequency and 120 sec in duration (120 twitch contractions). Target tension was controlled by changing the voltage of stimuli to obtain 100% twitch tension under buffer-perfused conditions (3–8 volts). Twitch tension was calculated as the average of a series

of contractions. Increasing the stimulation voltage in order to increase the contraction force recruits nerve fibers closest to the stimulating electrodes, and in reverse order, with large neurons that supply fast glycolytic muscle fibers being preferentially recruited.

Intracellular oxygenation

An NIRS instrument (NIRO-300 + Detection Fiber Adapter Kit, Hamamatsu Photonics, Shizuoka, Japan) was employed to measure oxygenation of Mb[9,10]. The distance between the photodiode and LED was fixed at 10 mm. NIRS probes were firmly attached to the skin of the gastrocnemius muscle and fixed by clamps on both sides of the muscle. During the initial period, for at least 30 sec before the onset of contraction, the average fluctuation in NIRS signals was adjusted to a zero reference value. After the exercise protocol, the anoxic buffer (equilibrated with 95% N_2 + 5% CO_2 gas) was perfused for 30 min to obtain maximal Mb desaturation. The equilibrium period with the anoxic buffer was initiated after 5 min recovery and after NIRS signals had returned to baseline. The NIRS signal attained steady state after 30 min. The muscle then received electrical stimulation so that it contracted for 2 min. No further increase in Δ[deoxy-Mb] signal was evident. The final Δ[deoxy-Mb] signal intensity served as the normalization constant for 100% Mb deoxygenation.

Data acquisition

The sampling rate for the NIRS data was 1 Hz. The other parameters (tension, perfusion pressure, O_2 content at inflow and outflow) were collected using a data acquisition system (PowerLab 8SP, AD Instruments, Castle Hill, Australia) at a sampling rate of 1 kHz. All data were transferred to a personal computer with acquisition software (Chart ver. 5.5.6, AD Instruments).

Data analysis

The data analysis followed our previous methods[9,12]. A simple moving average smoothed the Δ[deoxy-Mb] NIRS signals using a rolling average of 5 points, which corresponds to a 5 sec timeframe[14]. The Δ[deoxy-Mb] signals were calibrated against two different NIRS signal values: one at rest as 10% Mb deoxygenation and the other during steady state with anoxic buffer perfusion as 100% Mb deoxygenation. While the $S_{mb}O_2$ at rest could not be determined by NIRS, the value was assumed to be 90% based on previous studies reporting that the $S_{mb}O_2$ at rest was greater than 90%[11]. The %Δ[deoxy-Mb] plots were converted to $S_{mb}O_2$ (%) plots using the following equation:

$$S_{mb}O_2 = 100 - \%\Delta[\text{deoxy-Mb}]$$

$S_{mb}O_2$ plots were fitted by the following single-exponential equation to calculate kinetics parameters using an iterative least-squares technique by means of a commercial graphing/analysis package (KaleidaGraph 3.6.1, Synergy Software, Reading, PA, USA):

$$S_{mb}O_2 = BL + AP \times [1 - \exp^{-(t-TD)/\tau}]$$

where BL is the baseline value, AP the amplitude between BL and the steady-state value during the exponential component, TD the time delay between onset of contraction and appearance of $S_{mb}O_2$ signals, and τ the time constant of $S_{mb}O_2$ signal kinetics. Mean response time (MRT) calculated by TD + τ was used as an effective parameter of the response time for Mb deoxygenation at onset of muscle contraction. Dividing 63% of AP by MRT ($_{0.63}$AP/MRT) yields a value for Mb deoxygenation rate per unit time at the onset of exercise. The O_2 release rate from Mb was calculated using the following equation:

$$O_2 \text{ release rate from Mb} = (_{0.63}AP/MRT) \times [Mb] \times 60$$

where $_{0.63}$AP/MRT for $S_{mb}O_2$ was the Mb deoxygenation rate in %/sec. Inserting a value for [Mb] (Mb concentration) and multiplying by 60 seconds into the equation led to determination of the O_2 release rate from Mb in micromoles per gram per minute.

We reconstructed $P_{mb}O_2$ kinetics based on the resulting $S_{mb}O_2$ kinetics parameters. The model $S_{mb}O_2$ kinetics was converted to $P_{mb}O_2$ (mmHg) using the following equation:

$$P_{mb}O_2 = \frac{S_{mb}O_2 \cdot P_{50}}{(1 - S_{mb}O_2)}$$

where P_{50} is the partial oxygen pressure required to half-saturate Mb. A P_{50} of 2.4 mmHg was used for this equation, assuming a muscle temperature of 37°C[15]. The calculated $P_{mb}O_2$ plots were evaluated to obtain an MRT of its kinetics using the same single exponential equation as for $S_{mb}O_2$. The $_{0.63}$AP/MRT for $P_{mb}O_2$ indicates a rate of decrease in $P_{mb}O_2$ at muscle contraction onset. $P_{mb}O_2$ at steady state was calculated by using the $S_{mb}O_2$ value at steady state. Since O_2 partial pressure corresponds to a specific amount of dissolved O_2, intracellular [O_2] (μM) was calculated from the $P_{mb}O_2$ value at rest and at each O_2 condition using the following equation:

$$\text{Intracellular } [O_2] = P_{mb}O_2 \times O_2 \text{ solubility}$$

where $P_{mb}O_2$ is in mmHg, and O_2 solubility in buffer is 0.00135 μmol ml^{-1} $mmHg^{-1}$ at 37°C[16].

Muscle oxygen consumption

$m\dot{V}O_2$ was calculated from the arteriovenous O_2 content differential multiplied by flow rate, using the following:

$$m\dot{V}O_2 \text{ (μmol } g^{-1} \text{ } min^{-1}) = \text{flow rate} \times (PO_{2in} - PO_{2out}) \times O_2 \text{ solubility / muscle weight}$$

where flow rate is in milliliters per minute, and PO_{2in} and PO_{2out} are the arterial and venous oxygen tensions after

adjusting for water vapor pressure. Inflow and outflow PO_2 were measured continuously using two O_2 electrodes (5300A, YSI, Yellow Springs, Ohio, USA) along tubing before and after hindlimb perfusion. The vapor pressure at 37°C was 47.03 mmHg. The solubility of oxygen in the buffer was 0.00135 μmol per ml per mmHg at 37°C[16]. The $m\dot{V}O_2$ at rest and during muscle contraction was calculated by using values of $PO_{2in} - PO_{2out}$ averaged over 15 sec at steady state before and during muscle contraction.

Measurement of Mb concentration in buffer-perfused muscle tissue

After buffer perfusion, hindlimb muscles were isolated and weighed, thoroughly minced using stainless steel scissors, and homogenized in an ice bath with phosphate buffer (0.04 M, pH 6.6) bubbled with carbon monoxide (CO). The homogenate was then separated by centrifugation at 12,000 g for 30 min at 4°C. The clear supernatant was decanted into a microtube and again equilibrated with CO to ensure binding to Mb. The optical density at 538 nm (ß band) and 568 nm (α band) was employed for calculation of both Hb and Mb concentration in muscle tissue using a modified Reynafarje method[17].

Measurement of citrate synthase activity and mitochondrial respiration

Activity of citrate synthase (CS), a mitochondrial enzyme and marker of muscle oxidative potential, was measured in whole muscle homogenates using the spectrophotometric method described by Srere[18].

Mitochondria respiration was measured using an oxygen electrode via a modified method reported in a previous study[19]. For these measurements, an additional 15 Wistar male rats (n = 7 in Con group, n = 8 in IM group) were used, in addition to the animals used for the perfusion experiment. Briefly, the deep portion of the gastrocnemius muscle was minced using stainless steel scissors in the isolation medium and homogenized with a Potter–Elvehjem tissue grinder in the isolation medium at pH 7.2 at 4°C (225 mM mannitol, 100 mM KCl, 20 mM sucrose, 20 mM Hepes-2Na, 1 mM EDTA (ethylenediaminetetraacetic acid), 0.2% BSA (bovine serum albumin), 0.25 mg/mL proteinase, bacterial and 5 mM L-carnitine). The homogenized mixture was centrifuged at 700 g for 10 min at 4°C to remove nuclei and debris, and the supernatant was further centrifuged at 10,000 g for 10 min at 4°C to collect the isolated mitochondria. The mitochondrial pellet was washed once in the isolation medium and resuspended in a ratio of 0.4 μm per mg initial muscle weight with resuspension buffer at pH 7.2 at 4°C (215 mM mannitol, 75 mM Sucrose, 20 mM Hepes-2Na, 1 mM EDTA, 0.2% BSA and 5 mM L-carnitine). Mitochondrial respiration was monitored using a Clark-type oxygen electrode (Model-5300A, YSI Japan, Japan) at 37 °C in a thermostatically controlled chamber by adding 3 mL of reaction buffer (pH 7.2) at 37°C (225 mM mannitol, 75 mM sucrose, 20 mM Hepes-2Na, 10 mM KCl, 10 mM K_2HPO_4, 1 mM $MgCl_2$ $6H_2O$, 1 mM EDTA, 0.1% BSA and 5 mM L-carnitine) to it. After applying the substrate of pyruvate (5 mM) and L-malate (2 mM), 60 μL of isolated mitochondria under resuspension was added. After confirming that state 4 remained stable, ADP at the final concentration of 200 μM was added to the medium to initiate state 3.

Measurement of Mb expression in the mitochondrial fraction

The amount of Mb expression in the mitochondrial fraction was measured by western blotting according to previous studies[20-22]. In brief, the deep portion of the gastrocnemius muscle was homogenized in lysis buffer with the use of a loose-fitting Dounce homogenizer; then, the mitochondrial fraction was obtained by centrifuge separation method, as described in previous studies[21,22]. Western blot analysis was performed on the mitochondrial fraction in the deep portion of the gastrocnemius muscle. Equal amounts of protein samples were loaded onto 15% SDS-PAGE gels, and then transferred to a polyvinylidene fluoride (PDVF) membrane. The membrane was incubated in a blocking buffer and then with an anti-Mb antibody (sc-25607, Santa Cruz Biotechnology, CA, USA) and VDAC-I (ab15895, Abcam, UK) at 4°C overnight. It was then reacted with the secondary antibody, and the signals were visualized by enhanced chemiluminescence. The signal intensity was quantified with ImageJ imaging software.

Statistical analyses

All data were expressed as mean ± SD. An unpaired *t*-test was used to compare all biochemical and physiological parameters between groups. The level of significance was set at $p < 0.05$.

Results

The descriptive data for muscle weight are presented in Table 1. IM caused a significant, but uniform reduction in muscle mass [m. gastrocnemius 59%, m. plantaris 60%, m. soleus 63% and GPS (gastrocnemius-plantaris-soleus) 60%].

Table 2 summarizes the muscle tension, $m\dot{V}O_2$, and kinetics parameters for $S_{mb}O_2$ and $P_{mb}O_2$ at the maximal twitch tension level in both groups. The representative dynamics data of $S_{mb}O_2$ during muscle contraction in both groups are shown in Fig. 1. The maximal twitch tension in the IM group was significantly lower than in the Con group, whereas the $m\dot{V}O_{2peak}$ per gram per minute in the IM group during maximum twitch contraction was significantly higher than in the Con group, irrespective of the unchanged $m\dot{V}O_2$ at rest per gram per minute between both groups. When the efficiency of ATP synthesis was estimated by dividing the delta change in oxygen consumption during contraction by muscle tension, its value increased significantly in the IM compared to the

Table 1. Descriptive data for muscle weight

Parameter		Unit	Con	IM
Body Mass		g	275.0 ± 19.0	217.0 ± 21.8*
Muscle Mass	m. Gastrocnemius	mg	1805.8 ± 92.4	731.8 ± 44.9*
	m. Plantaris	mg	366.0 ± 26.7	147.2 ± 14.7*
	m. Soleus	mg	133.8 ± 16.9	49.2 ± 9.2*
	GPS	mg	2305.6 ± 129.1	928.2 ± 0.02*
GPS Mass /Body Mass		%	0.66 ± 0.03	0.34 ± 0.02*

Values are presented as mean ± SD (n = 6 in each group). Abbreviations: Con, control group; IM, immobilization group; GPS, gastrocnemius-plantaris-soleus; GPS mass/body mass, the ratio of GPS mass to body mass. The superscript (*) indicates a significant difference ($p < 0.05$ vs. Con).

Table 2. Muscle tension, muscle oxygen consumption, $S_{mb}O_2$ and $P_{mb}O_2$ kinetic parameters during muscle contraction

Parameter	Unit	Con	IM
Maximal Tension	g	91.0 ± 17.1	58.1 ± 6.5 *
$\dot{m}VO_2$ at rest	μmol g^{-1} min^{-1}	0.52 ± 0.14	0.66 ± 0.15
$\dot{m}VO_2$peak	μmol g^{-1} min^{-1}	0.74 ± 0.13	1.09 ± 0.19 *
$S_{mb}O_2$ Kinetics			
Steady-State Value	%	44.8 ± 11.9	62.5 ± 5.9 *
AP	%	-45.1 ± 11.9	-27.5 ± 6.0 *
MRT	s	41.2 ± 9.9	53.0 ± 9.7
$_{0.63}$AP/MRT	% s^{-1}	-0.73 ± 0.29	-0.33 ± 0.10 *
$P_{mb}O_2$ Kinetics			
Steady-State Value	mmHg	2.1 ± 1.0	4.2 ± 1.0 *
AP	mmHg	-19.4 ± 1.0	-17.5 ± 1.0 *
MRT	s	27.0 ± 3.6	37.2 ± 6.6 *
$_{0.63}$AP/MRT	mmHg s^{-1}	-0.45 ± 0.07	-0.30 ± 0.06 *

Values are mean ± SD (n = 6 in each group). Abbreviations: Con, control group; IM, immobilization group; AP, amplitude between BL (baseline) and the steady-state value during the exponential component; MRT, time required to reach 63% of AP from the onset of muscle contraction. $_{0.63}$AP/MRT is calculated by dividing $_{0.63}$AP by MRT. The superscript (*) indicates a significant difference ($p < 0.05$ vs. Con).

Con group (Con: 0.25 ± 0.11 vs. IM: 0.77 ± 0.25 10^{-2} μmol g_tissue^{-1} min^{-1} g_tension^{-1}; $p < 0.05$). With regard to the $S_{mb}O_2$ kinetic parameters, the steady-state value of $S_{mb}O_2$ kinetic parameters at the maximal twitch tension in the IM group was significantly higher than in the Con group, but AP and $_{0.63}$AP/MRT of the kinetic parameters for $S_{mb}O_2$ were lower. The MRT also tended to be longer at the maximal twitch tension. The all-kinetics parameters for $P_{mb}O_2$ showed significant differences in values between both groups. The steady state of $P_{mb}O_2$ and MRT showed higher values, and AP and $_{0.63}$AP/MRT showed lower values in the IM group.

Fig. 2 shows the comparison of the intracellular [O_2] (O_2 concentration) and the O_2 release rate from Mb at the maximal twitch tension between both groups. Intracellular [O_2] was based on $S_{mb}O_2$ - $P_{mb}O_2$ equilibrium. Muscle contraction resulted in a sharp decrease in intracellular O_2 from 29.2 μM at rest to 2.9 ± 1.7 and 5.6 ± 1.4 μM in the Con and IM groups, respectively, with significant differences in values between groups. The release rate of O_2 from Mb in the IM group showed a significant decrease compared to that of the Con group (Con: 7.5 ± 2.9 vs. IM: 3.2 ± 0.9 10^{-2} μmol g^{-1} min^{-1}; $p < 0.05$).

Fig. 3 shows isolated mitochondrial respiration rate

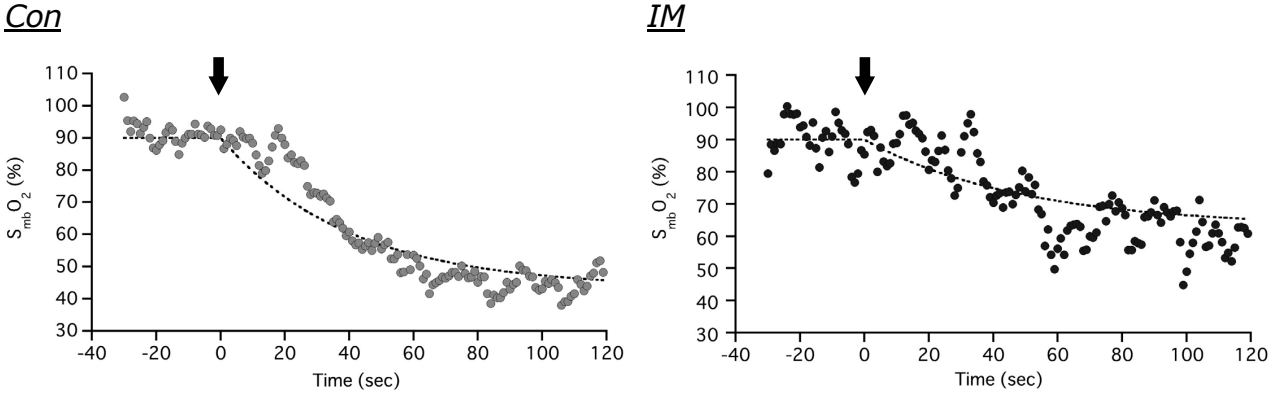

Fig. 1 Representative $S_{mb}O_2$ kinetics during muscle contraction at 1 Hz in control and immobilization groups.
The $S_{mb}O_2$ plots show representative data from a single experiment in each group. The $S_{mb}O_2$ kinetics in the representative immobilized rat declines with a mean response time (MRT) of 49.0 sec, while the $S_{mb}O_2$ kinetics in the representative control rat declines with an MRT of 40.0 sec. Because the NIRS device used in this experiment could not discriminate τ and TD of Mb deoxygenation kinetics due to the signal-to-noise ratio, the reconstructed exponential curve in both groups is fitted using an MRT (τ + TD) as the temporal parameter. The steady-state level of the representative immobilized rat during muscle contraction shows a higher level than in the representative control rat (immobilized rat: 63.0% vs. control rat: 43.4%). The black arrow shows the muscle contraction starting point, corresponding to 0 sec on the X-axis. Abbreviations: $S_{mb}O_2$, intracellular myoglobin saturation; NIRS, near-infrared spectroscopy; τ, time constant; TD, time delay.

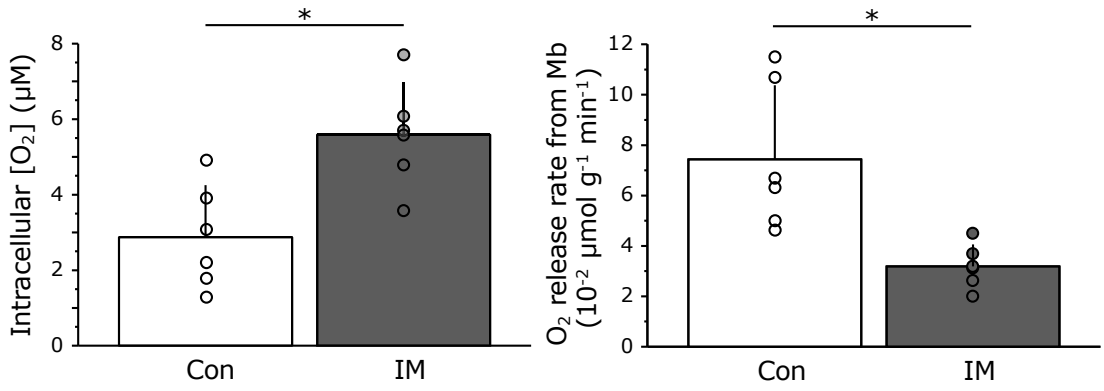

Fig. 2 Comparison of intracellular [O_2] and release rate of O_2 from Mb during maximal twitch contraction in control and immobilization groups.
While intracellular [O_2] (μM) during muscle contraction in the IM group was significantly higher than in the Con group, the release rate of O_2 from Mb at the onset of muscle contraction in the IM group was significantly lower than in the Con group. Values are represented as mean ± SD (n = 6 in each group). Abbreviations: Con, control group; IM, immobilization group; Mb, myoglobin. The superscript (*) indicates a significant difference ($p < 0.05$ vs. Con).

(state 4 and state 3), CS activity and Mb concentration between control and immobilized muscles. State 3 respiration was significantly decreased by IM, and state 4 respiration tended to be decreased as well. CS activity and Mb concentration did not show significant changes in response to IM. Additionally, the amount of Mb expression in the mitochondrial fraction remained unchanged by IM (Fig. 4).

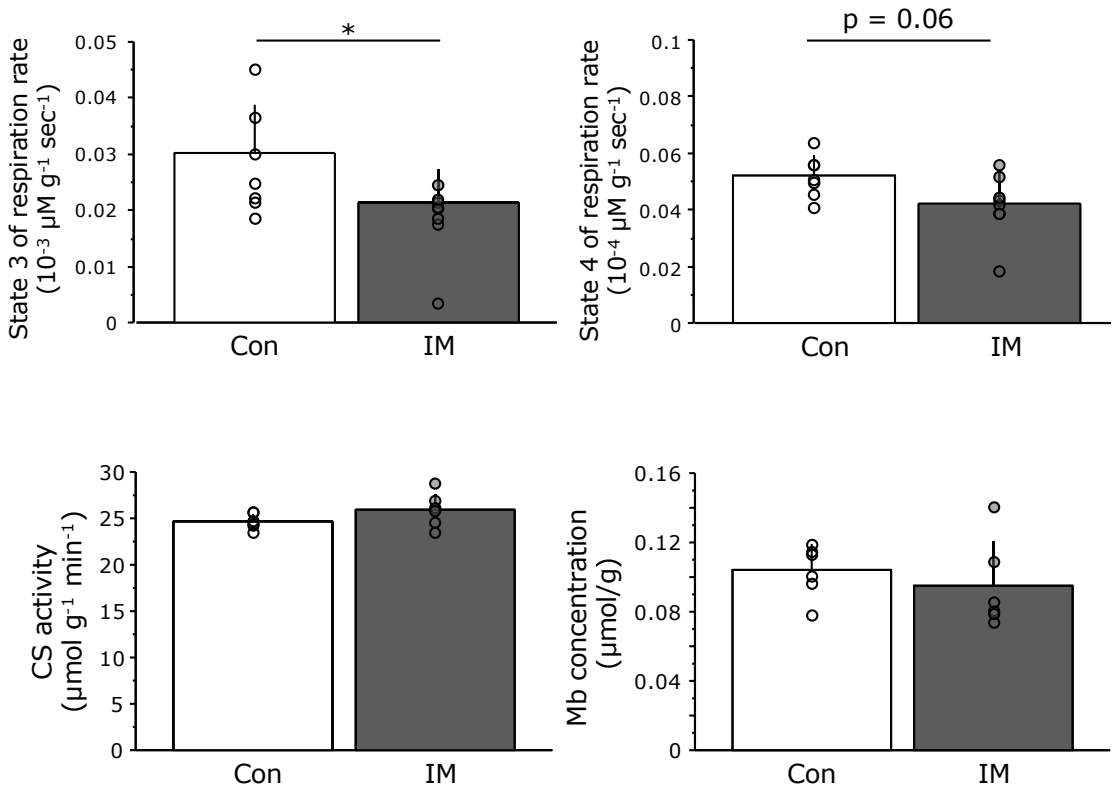

Fig. 3 Comparison of isolated mitochondria respiration capacity, CS activity and Mb concentration in control and immobilized skeletal muscle.
State 3 of mitochondrial respiration in IM group was significantly lower than in the Con group. State 4 in the IM group showed a tendency of being lower than in the Con group. CS activity and Mb concentration remained unchanged after the IM period. Values are represented as mean ± SD (n = 7 in Con group, n = 8 in IM group). Abbreviations: Con, control group; IM, immobilization group; CS, citrate synthase; Mb, myoglobin. The superscript (*) indicates a significant difference ($p < 0.05$ vs. Con).

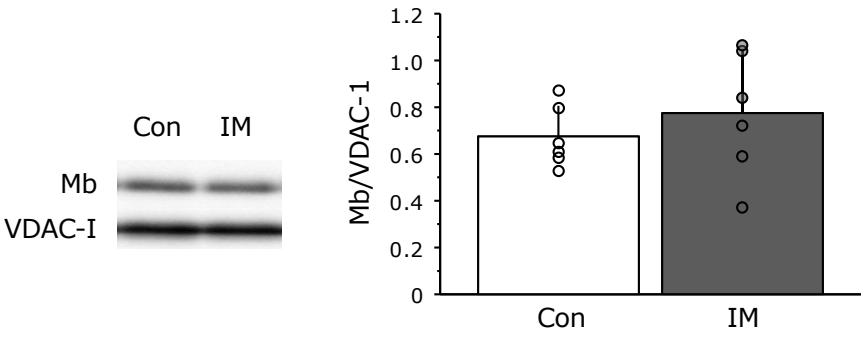

Fig. 4 Comparison of co-localization of Mb with mitochondria between immobilized and control skeletal muscle.
The amount of co-localization of Mb with mitochondria was unchanged by immobilization. Values are means ± SD (n = 6 in each group). Abbreviations: Con, control group; IM, immobilization group; Mb, myoglobin; VDAC-I, voltage-dependent anion channel-I.

Discussion

Three-week IM caused depletion in muscle mass and maximal twitch muscle tension by 60% and 36%, respectively. Although IM results in a wide range of adaptive responses in the skeletal muscle, muscle atrophy and decrease in muscle tension are the most pronounced characteristics of IM[23-25]. Conversely, the effect of IM on muscle oxygen metabolism and O_2 supply to the mitochondria during muscle contraction is not well documented and therefore, unclear. In the present study, CS activity, which reflects the mitochondrial content, was not affected after 3-week IM, whereas the mitochondrial function was attenuated. These phenomena are consistent with the reports on IM by Yajid et al.[5], who showed that 4 weeks of hindlimb suspension did not change CS activity in the gastrocnemius muscle, while the state 3 respiratory activity of isolated mitochondria quantitatively decreased when measured using pyruvate + malate as respiratory substrates. Taken together, the IM model used in the present study showed typical adaptation, and these observations suggest a reduction in mitochondrial oxidative phosphorylation potential in response to IM.

The present study has revealed a decrease in the O_2 release rate from Mb in the IM group, suggesting the possibility of a decrease in the mitochondrial respiration rate from resting to muscle contraction transition. Since mitochondrial respiration is accelerated without discernible delay after the onset of muscle contraction[26], O_2 flux to mitochondria must be increased nearly simultaneously. However, there were no changes in $P_{cap}O_2$ until 20 sec after the onset of muscle contraction[27]; therefore, the O_2 supply from Mb at this point significantly contributed to the abrupt increase in mitochondrial oxygen demand. Chung et al.[11] proposed the use of the Mb desaturation rate at the initiation of contraction as an index of cellular respiration, and myocyte experiments have also suggested that a direct Mb-mediated oxygen delivery might contribute to mitochondrial respiration[28]. The blockade of Mb oxygen-binding capacity suppressed approximately 70% of mitochondrial respiration, even under the conditions of sufficiently available O_2[28]. Conversely, overexpression of Mb improved muscle mitochondrial respiration via up-regulation of complex IV activity in cultured skeletal muscle cells (C2C12)[29]. These findings indicate that high or low Mb levels are one of the regulating factors for mitochondrial respiratory activity. However, as the Mb concentration remained unchanged after the IM period in this study, it should not have affected the mitochondrial respiratory capacity. Another regulating factor to consider is the positional relationship between Mb and mitochondria in the skeletal muscle. Since the basal partial pressure of O_2 (PO_2) in the myocardial and skeletal muscle cells *in vivo* was above 10 mmHg, the Mb translational diffusion in the cells appeared too slow to depend significantly on transport in the basal normoxic state[30-33]. In contrast, Mb desaturates immediately and rapidly in an exponential curve at the onset of muscle contraction and contributes to the oxygen supply to mitochondria[9]. Postnikova et al.[13] reported that the rate of Mb-O_2 deoxygenation for all mitochondrial states completely coincided with the rate of O_2 uptake by respiring mitochondria. Additionally, the O_2 release rate from Mb at a physiological PO_2 of 10–20 mmHg was possible only upon direct interaction with mitochondria[13,34]. Indeed, Yamada et al.[22] showed that Mb can interact directly with mitochondria and can co-localize with a mitochondrial complex. This phenomenon could have a potential significant role in mitochondrial respiration at the start of muscle contraction. If the amount of Mb expression in the mitochondrial fraction changes in the immobilized muscle, it could change the Mb kinetics at the onset of muscle contraction. However, such a change in the immobilized muscle was not present, as shown in Fig. 4. Therefore, since Mb concentration and the amount of Mb expression in the mitochondrial fraction remained unchanged after the IM period, the decrease in O_2 release rate from Mb is likely caused by a decreased mitochondrial respiratory capacity.

Recently, using simultaneous NMR and NIRS measurements, Bendahan et al.[35] also confirmed that Mb-O_2 released its O_2 within seconds at the start of a contraction to reach a new steady state level; the O_2 level fell progressively with increasing %MVC (maximal voluntary contraction), and the kinetics of Mb-O_2 desaturation observed using NMR and NIRS were matched, suggesting that Mb contributed predominantly to the NIRS signal from the muscle, especially during muscle contraction. Therefore, a delayed response of NIRS kinetics after the IM period should be caused by a change in Mb dynamics during muscle contraction, leading to a slower $\dot{V}O_2$ kinetics during exercise at the whole-body level.

Although IM led to an increase in $P_{mb}O_2$ during muscle contraction, $\Delta m\dot{V}O_2$ in the IM group was higher than in the Con group at the same relative twitch tension level. This result was inconsistent with our hypothesis that the higher $P_{mb}O_2$ during muscle contraction causes a decrease in O_2 gradient between extracellular and intracellular PO_2, resulting in a decrease in the $m\dot{V}O_2$ after IM. A putative explanation for the change in $m\dot{V}O_2$ may arise from a decreased coupling of ATP synthesis with O_2 uptake ratio (P/O). One mechanism for a decreased P/O may be an increased uncoupling of ATP resynthesis from O_2 consumption in skeletal muscles. Because a previous study reported that the coupling of ATP synthesis with O_2 uptake (P/O) decreased in aged muscles[36], the same phenomenon may occur in immobilized muscles. An increase in uncoupling protein 3 (*UCP3*) mRNA supports the possibility of decreased P/O in immobilized muscles[37]. Such an adaptation may reduce the electrical potential at the intermembrane space to alleviate the harmful effect due to the increase in reactive oxygen species owing to muscle inactivation. Therefore, an immobilized muscle needs to

consume more O_2 to meet the energetic demand of the tissue during muscle contraction.

Conversely, the higher $P_{mb}O_2$ cannot explain the increase in $m\dot{V}O_2$ during muscle contraction after the IM period. However, the oxygen level at the intracellular level alone does not determine the $m\dot{V}O_2$. The value of the $m\dot{V}O_2$ is dependent upon O_2 flux, as expressed in the following equation:

$$m\dot{V}O_2 = k \times DO_2 \times (P_{cap}O_2 - P_{mb}O_2)$$

where DO_2 is O_2 diffusion conductivity and $P_{cap}O_2$ is capillary PO_2.

As mentioned above, the increase in $m\dot{V}O_2$ could be attributed to the increased uncoupling of ATP resynthesis from O_2 uptake. In such cases, the increase in $m\dot{V}O_2$ requires increased O_2 flux, which would be achieved by increased DO_2. However, the factors involved in increased DO_2 remain obscure. One possibility might be the reduced diffusion distance during muscle atrophy. In previous studies, muscle atrophy due to IM did not alter DO_2 under isolated hindlimb perfusion[38,39]. However, since the degree of muscle atrophy in the present study (65% reduction in GPS muscle mass) was greater than in previous studies (32% reduction in gastrocnemius muscle[39]), the greater reduction in diffusion distance in our study might have caused the increased DO_2 in immobilized muscles, resulting in increased $m\dot{V}O_2$ during muscle contraction. In either event, the number of anastomotic capillaries tends to decrease in immobilized muscles; therefore, further careful observation is required to understand changes in oxygen diffusivity in muscle cells.

In conclusion, we studied the effect of IM on Mb dynamics during muscle contraction using a hindlimb perfusion model. The IM model used in this study showed the typical adaptation and caused a decrease in the release rate of O_2 from Mb at the onset of muscle contraction, which might have been associated with the altered mitochondrial respiration rate. These changes within muscle cells may be related to the delayed response of NIRS kinetics during muscle contraction. Further research is required to elucidate the mechanism of oxygen transport to mitochondria and the relationship between $P_{mb}O_2$ and $m\dot{V}O_2$ at the contraction phase in immobilized muscles.

Acknowledgements

This research was supported by a Grant-in-Aid for Scientific Research from the Japanese Ministry of Education, Science, Sports and Culture (20680032, 21650167, KM; 226926, HT), with partial support from the Yamaha Motor Foundation for Sports (KM) and the Nakatomi Foundation (KM).

Conflict of Interests

There is no conflict of interests for this study.

Author Contributions

HT, KM and TJ designed the research. HT, YF, and TY conducted the experiment and analyzed the data. HT wrote the manuscript and KM and TJ edited the paper. Finally, TH and SI helped with the experiments.

References

1) Berg HE, Dudley GA, Hather B and Tesch PA. 1993. Work capacity and metabolic and morphologic characteristics of the human quadriceps muscle in response to unloading. *Clin Physiol* 13: 337-347. doi: 10.1111/j.1475-097x.1993.tb00334.x.
2) Desplanches D. 1997. Structural and functional adaptations of skeletal muscle to weightlessness. *Int J Sports Med* 18 Suppl 4: S259-S264. doi: 10.1055/s-2007-972722.
3) Ferretti G, Antonutto G, Denis C, Hoppeler H, Minetti AE, Narici MV and Desplanches D. 1997. The interplay of central and peripheral factors in limiting maximal O_2 consumption in man after prolonged bed rest. *J Physiol* 501: 677-686. doi: 10.1111/j.1469-7793.1997.677bm.x.
4) Jackman RW and Kandarian SC. 2004. The molecular basis of skeletal muscle atrophy. *Am J Physiol Cell Physiol* 287: C834-C843. doi: 10.1152/ajpcell.00579.2003.
5) Yajid F, Mercier JG, Mercier BM, Dubouchaud H and Prefaut C. 1998. Effects of 4 wk of hindlimb suspension on skeletal muscle mitochondrial respiration in rats. *J Appl Physiol* 84: 479-485. doi: 10.1152/jappl.1998.84.2.479.
6) Convertino VA, Goldwater DJ and Sandler H. 1984. $\dot{V}O_2$ kinetics of constant-load exercise following bed-rest-induced deconditioning. *J Appl Physiol Respir Environ Exerc Physiol* 57: 1545-1550. doi: 10.1152/jappl.1984.57.5.1545.
7) Furuichi Y, Masuda K, Takakura H, Hotta N, Ishida K, Katayama K, Iwase S and Akima H. 2009. Effect of intensive interval training during unloading on muscle deoxygenation kinetics. *Int J Sports Med* 30: 563-568. doi: 10.1055/s-0029-1202824.
8) Kitahara A, Hamaoka T, Murase N, Homma T, Kurosawa Y, Ueda C, Nagasawa T, Ichimura S, Motobe M, Yashiro K, Nakano S and Katsumura T. 2003. Deterioration of muscle function after 21-day forearm immobilization. *Med Sci Sports Exerc* 35: 1697-1702. doi: 10.1249/01.MSS.0000089339.07610.5F.
9) Takakura H, Masuda K, Hashimoto T, Iwase S and Jue T. 2010. Quantification of myoglobin deoxygenation and intracellular partial pressure of O_2 during muscle contraction during haemoglobin-free medium perfusion. *Exp Physiol* 95: 630-640. doi: 10.1113/expphysiol.2009.050344.
10) Masuda K, Takakura H, Furuichi Y, Iwase S and Jue T. 2010. NIRS measurement of O_2 dynamics in contracting blood and buffer perfused hindlimb muscle. *Adv Exp Med Biol* 662: 323-328. doi: 10.1007/978-1-4419-1241-1_46.
11) Chung Y, Molé PA, Sailasuta N, Tran TK, Hurd R and Jue T. 2005. Control of respiration and bioenergetics during muscle contraction. *Am J Physiol Cell Physiol* 288: C730-C738. doi: 10.1152/ajpcell.00138.2004.
12) Takakura H, Furuichi Y, Yamada T, Jue T, Ojino M, Hashimoto T, Iwase S, Hojo T, Izawa T and Masuda K. 2015. Endurance training facilitates myoglobin desaturation during muscle contraction in rat skeletal muscle. *Sci Rep* 5: 9403.

doi: 10.1038/srep09403.
13) Postnikova GB, Tselikova SV and Shekhovtsova EA. 2009. Myoglobin and mitochondria: oxymyoglobin interacts with mitochondrial membrane during deoxygenation. *Biochemistry (Mosc)* 74: 1211-1218. doi: 10.1134/s0006297909110054.
14) Box GEP, Hunter WG and Hunter JS. 1978. *Statistics for Experimenters: An Introduction to Design, Data Analysis, and Model Building*. John Wiley & Sons, New York.
15) Schenkman KA, Marble DR, Burns DH and Feigl EO. 1997. Myoglobin oxygen dissociation by multiwavelength spectroscopy. *J Appl Physiol* 82: 86-92. doi: 10.1152/jappl.1997.82.1.86.
16) Philip LA and Dorothy SD. 1971. *Respiration and Circulation*. Federation of American Societies for Experimental Biology, Bethesda, MD.
17) Masuda K, Truscott K, Lin PC, Kreutzer U, Chung Y, Sriram R and Jue T. 2008. Determination of myoglobin concentration in blood-perfused tissue. *Eur J Appl Physiol* 104: 41-48. doi: 10.1007/s00421-008-0775-x.
18) Srere PA. 1969. Citrate synthase. *Methods Enzymol* 13: 3-11. doi: 10.1016/0076-6879(69)13005-0.
19) Oyanagi E, Yano H, Uchida M, Utsumi K and Sasaki J. 2011. Protective action of L-carnitine on cardiac mitochondrial function and structure against fatty acid stress. *Biochem Biophys Res Commun* 412: 61-67. doi: 10.1016/j.bbrc.2011.07.039.
20) Furuichi Y, Sugiura T, Kato Y, Shimada Y and Masuda K. 2010. OCTN2 is associated with carnitine transport capacity of rat skeletal muscles. *Acta Physiol (Oxf)* 200: 57-64. doi: 10.1111/j.1748-1716.2010.02101.x.
21) Hashimoto T, Hussien R and Brooks GA. 2006. Colocalization of MCT1, CD147, and LDH in mitochondrial inner membrane of L6 muscle cells: evidence of a mitochondrial lactate oxidation complex. *Am J Physiol Endocrinol Metab* 290: E1237-E1244. doi: 10.1152/ajpendo.00594.2005.
22) Yamada T, Furuichi Y, Takakura H, Hashimoto T, Hanai Y, Jue T and Masuda K. 2013. Interaction between myoglobin and mitochondria in rat skeletal muscle. *J Appl Physiol* 114: 490-497. doi: 10.1152/japplphysiol.00789.2012.
23) Booth FW. 1982. Effect of limb immobilization on skeletal muscle. *J Appl Physiol* 52: 1113-1118. doi: 10.1152/jappl.1982.52.5.1113.
24) Cooper RR. 1972. Alterations during immobilization and regeneration of skeletal muscle in cats. *J Bone Joint Surg Am* 54: 919-953.
25) Eisenhauer J and Key JA. 1945. Studies on muscle atrophy: a method of recording power in situ and observations on effect of position of immobilization on atrophy of disuse and denervation. *Arch Surg* 51: 154-163.
26) Balaban RS, Bose S, French SA and Territo PR. 2003. Role of calcium in metabolic signaling between cardiac sarcoplasmic reticulum and mitochondria in vitro. *Am J Physiol Cell Physiol* 284: C285-C293. doi: 10.1152/ajpcell.00129.2002.
27) Behnke BJ, Kindig CA, Musch TI, Koga S and Poole DC. 2001. Dynamics of microvascular oxygen pressure across the rest-exercise transition in rat skeletal muscle. *Respir Physiol* 126: 53-63. doi: 10.1016/s0034-5687(01)00195-5.
28) Wittenberg BA and Wittenberg JB. 1987. Myoglobin-mediated oxygen delivery to mitochondria of isolated cardiac myocytes. *Proc Natl Acad Sci USA* 84: 7503-7507. doi: 10.1073/pnas.84.21.7503.
29) Yamada T, Takakura H, Jue T, Hashimoto T, Ishizawa R, Furuichi Y, Kato Y, Iwanaka N and Masuda K. 2016. Myoglobin and the regulation of mitochondrial respiratory chain complex IV. *J Physiol* 594: 483-495. doi: 10.1113/JP270824.
30) Kreutzer U, Mekhamer Y, Tran TK and Jue T. 1998. Role of oxygen in limiting respiration in the in situ myocardium. *J Mol Cell Cardiol* 30: 2651-2655. doi: 10.1006/jmcc.1998.0823.
31) Lin PC, Kreutzer U and Jue T. 2007. Myoglobin translational diffusion in rat myocardium and its implication on intracellular oxygen transport. *J Physiol* 578: 595-603. doi: 10.1113/jphysiol.2006.116061.
32) Molé PA, Chung Y, Tran TK, Sailasuta N, Hurd R and Jue T. 1999. Myoglobin desaturation with exercise intensity in human gastrocnemius muscle. *Am J Physiol* 277: R173-R180. doi: 10.1152/ajpregu.1999.277.1.R173.
33) Zhang J, Murakami Y, Zhang Y, Cho YK, Ye Y, Gong G, Bache RJ, Ugurbil K and From AH. 1999. Oxygen delivery does not limit cardiac performance during high work states. *Am J Physiol* 277: H50-H57. doi: 10.1152/ajpheart.1999.277.1.H50.
34) Postnikova GB and Tselikova SV. 2005. Myoglobin and mitochondria: kinetics of oxymyoglobin deoxygenation in mitochondria suspension. *Biofizika* 50: 297-306.
35) Bendahan D, Chatel B and Jue T. 2017. Comparative NMR and NIRS analysis of oxygen-dependent metabolism in exercising finger flexor muscles. *Am J Physiol Regul Integr Comp Physiol* 313: R740-R753. doi: 10.1152/ajpregu.00203.2017.
36) Marcinek DJ, Schenkman KA, Ciesielski WA, Lee D and Conley KE. 2005. Reduced mitochondrial coupling in vivo alters cellular energetics in aged mouse skeletal muscle. *J Physiol* 569: 467-473. doi: 10.1113/jphysiol.2005.097782.
37) Andrianjafiniony T, Dupre-Aucouturier S, Letexier D, Couchoux H and Desplanches D. 2010. Oxidative stress, apoptosis, and proteolysis in skeletal muscle repair after unloading. *Am J Physiol Cell Physiol* 299: C307-C315. doi: 10.1152/ajpcell.00069.2010.
38) Bebout DE, Hogan MC, Hempleman SC and Wagner PD. 1993. Effects of training and immobilization on $\dot{V}O_2$ and DO_2 in dog gastrocnemius muscle in situ. *J Appl Physiol* 74: 1697-1703. doi: 10.1152/jappl.1993.74.4.1697.
39) Hepple RT, Hogan MC, Stary C, Bebout DE, Mathieu-Costello O and Wagner PD. 2000. Structural basis of muscle O_2 diffusing capacity: evidence from muscle function in situ. *J Appl Physiol* 88: 560-566. doi: 10.1152/jappl.2000.88.2.560.